

SLITHERING LOCOMOTION

DAVID L. HU(✉)^{||} AND MICHAEL SHELLEY^{**}

Abstract. Limbless terrestrial animals propel themselves by sliding their bellies along the ground. Although the study of dry solid-solid friction is a classical subject, the mechanisms underlying friction-based limbless propulsion have received little attention. We review and expand upon our previous work on the locomotion of snakes, who are expert sliders. We show that snakes use two principal mechanisms to slither on flat surfaces. First, their bellies are covered with scales that catch upon ground asperities, providing frictional anisotropy. Second, they are able to lift parts of their body slightly off the ground when moving. This reduces undesired frictional drag and applies greater pressure to the parts of the belly that are pushing the snake forwards. We review a theoretical framework that may be adapted by future investigators to understand other kinds of limbless locomotion.

Key words. Snakes, friction, locomotion

AMS(MOS) subject classifications. Primary 76Zxx

1. Introduction. Animal locomotion is as diverse as animal form. Swimming, flying and walking have received much attention [1, 9] with the latter being the most commonly studied means for moving on land (Fig. 1). Comparatively little attention has been paid to limbless locomotion on land, which necessarily relies upon sliding. Sliding is physically distinct from pushing against a fluid and understanding it as a form of locomotion presents new challenges, as we present in this review.

Terrestrial limbless animals are rare. Those that are multicellular include worms, snails and snakes, and account for less than 2% of the 1.8 million named species (Fig. 1). Many are long as well as flexible, enabling them to enter crevices of dimension much smaller than their body length [43]. Such creatures can slither over or burrow through mechanically complex environments such as sand [29], soil [40], grass, or the insides of other organisms such as their intestines or muscle tissue. Investigators are studying locomotion through other complex media, such as viscoelastic or wet granular materials (see [12, 25, 26, 41] and references therein). Snails and many worms propel themselves by virtue of using wet surfaces [7]. Conversely, terrestrial snakes rely upon dry solid-solid friction for propulsion.

Avoiding a harmful tumble or fall is a requirement for moving on land. Because their heights are at most a few centimeters, limbless locomotors have a short gravitational time scale of falling $\tau = \sqrt{L/g} \sim 0.3$ s. An outstretched and unconscious snake can thus easily be rolled onto its back.

^{||}School of Mechanical Engineering, Georgia Institute of Technology, Atlanta, GA 30318, USA

^{**}Courant Institute of Mathematical Sciences, New York University, New York, NY, USA

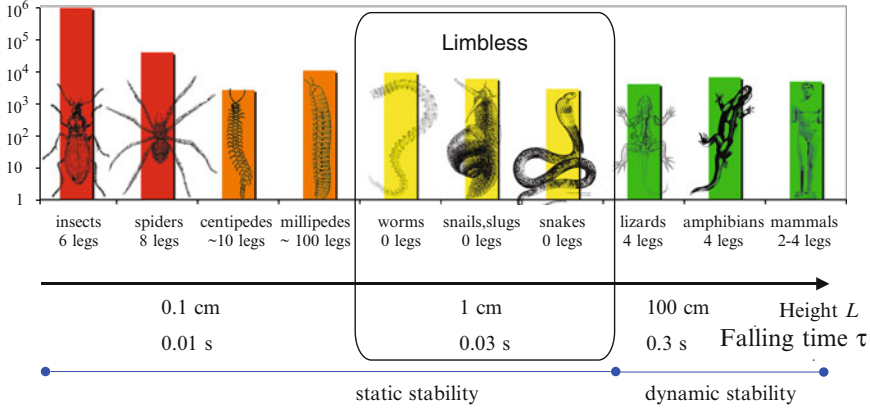


FIG. 1. Classes of terrestrial animals, arranged according to their size and number of identified species

To avoid flipping over, they tend to keep their bodies sprawled, such as in the familiar S-shape during slithering. Smaller organisms like the insects maintain stability using their many legs. Larger organisms have sufficient falling time that they may rely on the use of limbs and on gaits such as the trot or gallop, in which an airborne phase occurs. Such is rare for limbless organisms.

One reason for the rarity of limbless organisms may be the cost of abrasion due to sliding against the ground. This is less of a problem for legged organisms, which are in static contact via hard materials such as hooves and nails. A material's resistance to wear is characterized by a wear coefficient $k = V/(ND)$ where V is the volume of the material worn after sliding a distance D under an applied normal force N [42]. Our measurements of the sloughed skin of a 30-cm corn snake and a 2-m red-tailed boa indicate that their skin thicknesses are comparable (0.05 mm). Snakes do not heal their skin, but instead shed and replace their skin periodically. If snake skin thickness is a constant across snakes, then the volume V of the belly skin scales as the surface area of the belly. Therefore, the maximum distance a snake of length L can travel before wearing away its ventral skin scales as $D \sim V/Nk \sim L^2/L^3 \sim L^{-1}$. This scaling indicates that the maximum distance that snakes can travel is inversely proportional to their length, making wear avoidance an important constraint for large snakes.

1.1. Snakes: Movement Using Dry Solid–Solid Friction.

Snakes, suborder *Serpentes*, are the most successful class of non-microscopic terrestrial limbless organisms. Numbering over 2,900 species, they have evolved to occupy two orders of magnitude in length-scale, from 10-cm threadsnakes to 10-m long anacondas (Fig. 2). All possess the same basic

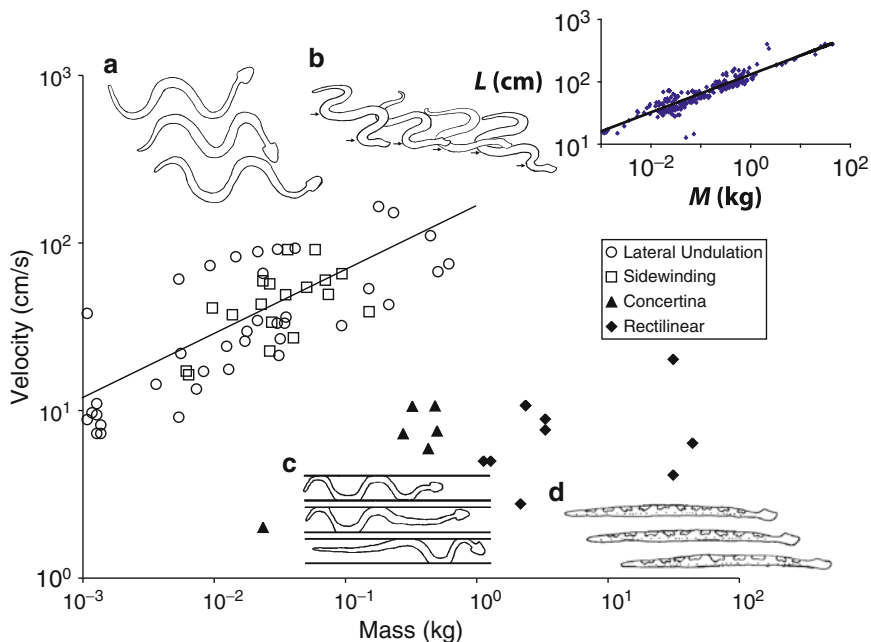


FIG. 2. The relation between maximum speed U and body mass M for 140 specimens of snakes. The fit line suggests that $U \sim M^{1/3}$. The inset, showing the relation between mass M and length L , indicates that snakes are isometric: $M \sim L^3$. Taken together, this suggests that $U \sim L$. Snake modes of locomotion are shown in the insets: (a) lateral undulation or slithering involving two-dimensional undulation; (b) Sidewinding, resulting from helical motion; (c) Concertina motion. (d) Rectilinear progression resulting from contraction and extension along a single axis. Anatomical and kinematic measurements were compiled from existing data [13, 16, 21, 24, 27, 32, 35, 38, 39]

body design: A flexible tube of tissue and skeleton covered in hardened scales (Fig. 3b). Moreover, our measurements indicate that their bodies are isometric, meaning that their proportions are generally independent of size (inset of Fig. 2). Their body form lends them tremendous versatility: They can slither up tree trunks, transition from slithering to swimming without changing gait, or slither across land with surprising rapidity (the red racer [34] of length 60–135 cm can slither at speeds of 130 cm/sec). Such abilities make snakes the champions of terrestrial limbless locomotion.

Limbed animals such as horses have several gaits, such as the walk, trot and gallop [1]. They will readily change gaits in turn as they increase speed, analogous to a car changing gears. We can also ascribe to snakes four principal “gaits”, according to the pattern of placements of their limbless body on the ground. They are the undulatory gaits (involving traveling waves) and the ratcheting gaits (involving extensile-contractile motions) (Fig. 2a–d; [3, 11, 15, 17, 24, 33]). The most common is lateral undulation, or sinuous slithering, in which the body propagates a 2-D traveling wave from head to tail, in the manner of a swimming eel. The addition

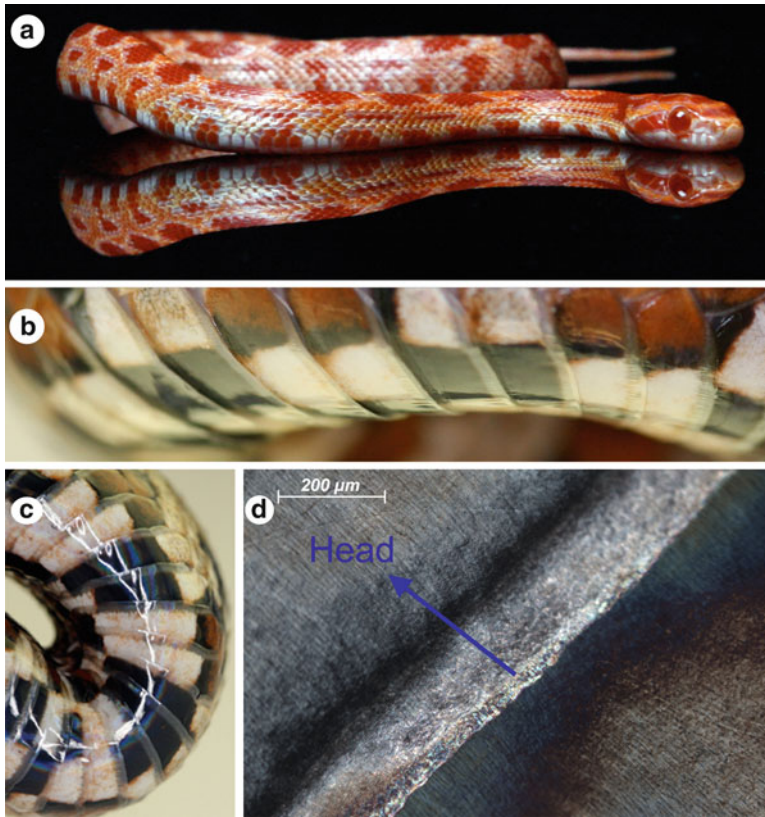


FIG. 3. (a) A corn snake lifting its body while slithering on a mirrored surface. (b) The ventral scales of the corn snake. Snakeskin adheres to, and folds in and out of, the overlapping lamellae, forming a directionally anisotropic frictional surface. Friction is least when sliding from head to tail, and greatest when sliding towards the flanks. (c), Bending by the snake causes the scales to fan radially outward like a fan, also locally increasing lateral friction. (d) Close-up of the edge of a scale shows micro-ridges that may increase lateral friction

of a vertical traveling wave to this gait yields a helical body motion called sidewinding, whereby snakes roll along like wheels without axles, and rely on static contact similar to walking. A snake may also progress rectilinearly in the manner of worms by one-dimensional contraction and extension of its belly muscles. Finally, by folding laterally like a sheet of paper, a snake may progress in an accordion-like fashion referred to as concertina. Unlike horses, snake gaits are not so directly related to body speed. Snakes will transition between these gaits in turn as the friction coefficient with the underlying surface is increased [38]. Choice of gait also appears to depend on other factors, such as their body type and the surrounding terrain conditions (flat ground or narrow passageways). In modeling of snake

locomotion, we hope to ultimately understand the underlying mechanical reasons (stability, speed, efficiency) leading to the snake's choice of gait.

An attractive feature of limbless locomotion is that its cost of transport is no greater than that of limbed animals. Oxygen consumption is used to measure the energetic net cost of transport (NCT), which has units of energy consumed per mass of animal per distance travelled. By measuring the oxygen consumption of snakes on treadmills, Walton et al. [44] found that the NCT of a slithering snake is 23 J/kg m, which is near that of a similarly-sized running mammal or bird. This result drew attention in its time because biologists had hypothesized that snakes should have a lower NCT than legged organisms because of their energetic savings due to a lower height and lower inertial losses from swinging limbs. Evidently, the frictional costs of sliding trump these gains.

Further treadmill studies by Secor [39] showed that sidewinding has an NCT of 8 J/kg m. Combining the results of Secor and Walton et al., Alexander [1] reports a hierarchy of snake efficiencies: Sidewinding is most efficient, with nearly a third the NCT of lateral undulation; concertina is the least efficient (170 J/kg m) with nearly seven times the NCT of lateral undulation. The NCT of rectilinear motion has yet to be measured. These measurements suggest that future snake robots may have the same efficiencies as legged ones.

The reported efficiencies are reflected in the maximum speeds associated with each gait. The regime diagram Fig. 2 shows the relation between snake speed U and body mass M for 140 species of snakes. Each limbless gait occupies a distinct region in the speed-weight parameter space. Among the undulatory gaits, we find that snake speed scales with body length: $U \sim M^{1/3} \sim L$. This is distinct from Froude's Law ($U \sim L^{1/2}$), known for birds and fish [6]. Presumably, this difference results from the use of frictional rather than fluid dynamic forces. As yet no supporting theoretical models explain these trends.

Size is the clearest indicator of what gait the snake will use. As shown in Fig. 2, snakes lighter than $M \approx 1$ kg prefer undulatory gaits, while those heavier generally prefer ratcheting. One reason for this is the diminishing force-to-weight ratio of animals with increasing size. For a snake to propel itself from rest, it must overcome the static friction force $F_f = \mu Mg \sim L^3$ where μ is the coefficient of static friction and $M \sim L^3$ is due to isometry (Fig. 2 inset). The maximum force a snake can generate scales as $F_{max} \sim \sigma L^2$, the product of the peak muscular stress σ and the cross-sectional area of its muscles, which for an isometric snakes, scales as L^2 . Small snakes with $F_{max} > F_f$ have no problems slithering, and are quick to escape if startled. However, a sufficiently large snake, for which $L^2 < (\mu g / \sigma) L^3$, only musters enough strength to move individual parts of its body at-a-time, rather than simultaneously. Thus, the largest snakes would tend to use concertina or rectilinear motion to move, which they do.

1.2. Previous Snake Motion Modeling. Models of snake locomotion are generally idealized, without taking directional differences in sliding friction fully into account [19, 28, 37]. Many were developed as part of motion-planning schemes for wheeled snake-robots [5, 8, 10, 22, 31, 36]. These models rely on the high frictional anisotropy provided by passive wheels beneath the body. Despite their reliance on wheels, these models work well to describe the motion of snakes slithering through arrays of rocks, which act as lateral push-points. However snakes may also encounter natural planar surfaces such as bare rock or sand without adequate push-points. Over such surfaces, sliding friction and the frictional properties of snake scales need to be considered [18, 20].

In 2009, we tested unconscious snakes and found that on sufficiently rough surfaces, like stretched cloth, the snakes' overlapping ventral scutes gave them a preferred direction of sliding [23]. Sliding is resisted most in the lateral direction, where snake scales catch in asperities of the underlying surface (Fig. 3b). Using a theoretical model (Fig. 3c), we showed that the level of frictional anisotropy presented by the snake's scales, when coupled with the snake's motion kinematics (undulation and lifting), was sufficient to predict some of the observed snake speeds. We note that our friction measurements were done with unconscious snakes that were laid out straight. As is discussed in the caption of Fig. 3 and in the Discussion, lateral friction is likely increased by bending of the snake body and by active control of individual scales [30].

In the following, we provide a more extensive presentation of our theoretical work. In Sect. 2, we introduce our experimental measurements of sliding resistance in snakes. In Sect. 3, we present our theoretical model based on our friction measurements. We follow in Sect. 4 with descriptions of the snake body-lifting and how lifting augments the body speed. In Sect. 5, we present the implications of our work and suggestions for future work.

2. Snake Experiments. We performed experiments with juvenile milk and corn snakes (methods described in our previous work [23]). We crudely characterize our system by snake length $L = 30$ cm, period of undulation $\tau = 2$ s, mass per unit length ρ and measured friction coefficients $\mu_f = 0.11$, $\mu_b = 0.14$, $\mu_t = 0.19$ associated with the snake sliding in the forward, backwards and transverse directions (see [23] and Fig. 4). The forces available to the snake include inertia, scaling as $\rho L^2/\tau^2$, gravitational force ρg , and friction in three directions in the plane, which we scale as $\mu_f \rho g L$ where μ_f is the coefficient of friction for forward sliding. The relative magnitudes of these forces are calculated using corn and milk snake experiments on cloth:

$$\mu_f = \frac{\text{forward friction}}{\text{gravity}} \sim 0.11$$

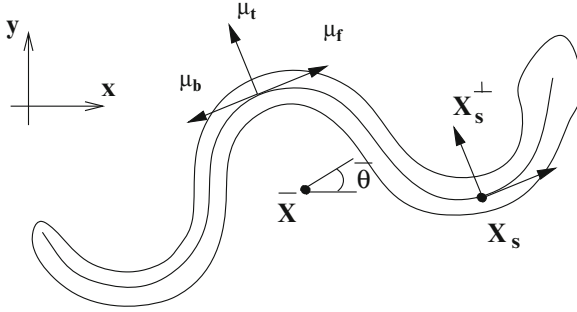


FIG. 4. Schematic diagram for our theoretical model, where \bar{X} denotes the snake's center of mass, θ its mean orientation, and \hat{s} and \hat{n} the tangent (pointing towards the head) and normal vectors to the body (Taken from Hu et al. [23])

$$Fr = \frac{L}{\mu_f g \tau^2} = \frac{\text{inertia}}{\text{friction}} \sim 10^{-3} \quad (1)$$

$$An_{\parallel} = \frac{\mu_b}{\mu_f} = \frac{\text{backward friction}}{\text{forward friction}} \sim 1.3$$

$$An_{\perp} = \frac{\mu_t}{\mu_f} = \frac{\text{transverse friction}}{\text{forward friction}} \sim 1.7.$$

These values will vary according to snake species and surface of choice. We note that for corn and milk snakes on cloth, the frictional anisotropies (An_{\perp} and An_{\parallel}) are comparable. For most surfaces, the Froude number Fr is small, indicating that frictional (and gravitational) forces are greatly in excess of inertial forces. Physically this means that snakes do not need “brakes,” to decelerate on horizontal surfaces: Cessation of slithering will cause them to quickly come to a halt. When in motion, the most important ratio governing speed is the transverse-to-forward frictional anisotropy $An_{\perp} = \mu_t/\mu_f$. This is the ratio of a snake's resistance to sliding sideways versus sliding towards its head.

We observed that snakes move best on surfaces that provide low abrasion to the snake, but sufficient roughness so that the scales can “catch” and provide frictional anisotropy. We ultimately settled upon 2 test materials for our experiments. The first is a cloth whose stitches are such that the characteristic length scale of roughness (0.2 mm) is comparable with the thickness of the snakes belly scales (0.1 mm). The second is a smooth fiberboard (table top), whose scale of roughness 20 μm is one-fifth that of the snakes scales. For milk snakes on cloth, the transverse-to-forward anisotropy is approximately 2; on smoother fiberboard, it is nearly unity. Higher anisotropy values ($An_{\perp} = 10$) can be achieved by employing wheels, as is done in snake robots [22].

3. The Kinematic Snake Model. We present here a simple kinematic model of serpentine lateral undulation, originally reported in our study [23]. The virtual snake, shown in Fig. 4, is modeled as an inextensible one-dimensional curve $\mathbf{X}(s, t) = (x(s, t), y(s, t))$ of length L ($0 \leq s \leq L$) and mass per unit length ρ , here taken as uniform. We describe the shape and dynamics of the snake in terms of its curvature, $\kappa(s, t)$, that is, without reference to absolute position or orientation. Given κ , the position and orientation are given by simple planar geometric relations,

$$\begin{aligned}\mathbf{X}(s, t) &= \bar{\mathbf{X}}(t) + I_0[\mathbf{X}_s](s, t) \\ \theta(s, t) &= \bar{\theta}(t) + I_0[\kappa](s, t)\end{aligned}\quad (2)$$

where $\mathbf{X}_s = (\cos \theta, \sin \theta)$ is the unit tangent vector, θ is the tangent angle to the x-axis, and I_0 the mean-zero antiderivative of its argument.¹ Hence $\bar{\mathbf{X}}$ is the center of mass and $\bar{\theta}$ is the average orientation. The normal vector is given by $\mathbf{X}_s^\perp = (-\sin \theta, \cos \theta)$ where $(x, y)^\perp = (-y, x)$.

Taking a derivative with respect to time yields

$$\begin{aligned}\mathbf{X}_t &= \dot{\bar{\mathbf{X}}} + I_0[\mathbf{X}_s^\perp \theta_t] \\ \theta_t &= \dot{\bar{\theta}} + I_0[\kappa_t],\end{aligned}\quad (3)$$

or

$$\mathbf{X}_t = \dot{\bar{\mathbf{X}}} + I_0 \left[\mathbf{X}_s^\perp (\dot{\bar{\theta}} + I_0[\kappa_t]) \right]. \quad (4)$$

Taking another derivative yields

$$\mathbf{X}_{tt} = \ddot{\bar{\mathbf{X}}} + I_0 \left[-\mathbf{X}_s (\dot{\bar{\theta}} + I_0[\kappa_t])^2 \right] + I_0 \left[\mathbf{X}_s^\perp (\ddot{\bar{\theta}} + I_0[\kappa_{tt}]) \right]. \quad (5)$$

By Newton's second law, the dynamics of the snake is prescribed by the point-wise force balance,

$$\rho \mathbf{X}_{tt}(s, t) = \mathbf{F}(s, t) + \mathbf{f}(s, t) \quad (6)$$

where \mathbf{F} and \mathbf{f} are the external and internal forces per unit length, respectively. We assume that the total internal forces and torques are zero:

$$\int_0^L \mathbf{f} \, ds = 0 \quad \text{and} \quad \int_0^L (\mathbf{X} - \bar{\mathbf{X}})^\perp \cdot \mathbf{f} \, ds = 0. \quad (7)$$

External forces on the snake are given entirely by frictional forces acting on its ventral surface. We neglect static friction and address the validity

¹ $I_0[f](s, t) = \int_0^s f(s', t) ds' - \frac{1}{L} \int_0^L ds \int_0^s ds' f(s, t).$

of this assumption in our results section. We use a sliding friction law that builds in the measured directionally anisotropic friction in the forward (\mathbf{X}_s), backwards ($-\mathbf{X}_s$), and lateral directions (\mathbf{X}_s^\perp) relative to the local direction of motion $\hat{\mathbf{u}} = \mathbf{X}_t(s, t)/|\mathbf{X}_t(s, t)|$:

$$\begin{aligned} \mathbf{F} = & -\rho g \left(\mu_t (\hat{\mathbf{u}} \cdot \mathbf{X}_s^\perp) \mathbf{X}_s^\perp \right. \\ & \left. + \left[\mu_f H(\hat{\mathbf{u}} \cdot \mathbf{X}_s) + \mu_b (1 - H(\hat{\mathbf{u}} \cdot \mathbf{X}_s)) \right] (\hat{\mathbf{u}} \cdot \mathbf{X}_s) \mathbf{X}_s \right) \end{aligned} \quad (8)$$

where the Heaviside step function $H = \frac{1}{2}[1 + \text{sgn}(x)]$ is used to distinguish the components in the \mathbf{X}_s and $-\mathbf{X}_s$ direction.

Scaling \mathbf{X} on L , t on the undulation period τ , and the internal force \mathbf{f} on ρg , we have

$$\begin{aligned} Fr \mathbf{X}_{tt} = \mathbf{f} - & \left(\mu_t (\hat{\mathbf{u}} \cdot \mathbf{X}_s^\perp) \mathbf{X}_s^\perp + \left[\mu_f H(\hat{\mathbf{u}} \cdot \mathbf{X}_s) \right. \right. \\ & \left. \left. + \mu_b (1 - H(\hat{\mathbf{u}} \cdot \mathbf{X}_s)) \right] (\hat{\mathbf{u}} \cdot \mathbf{X}_s) \mathbf{X}_s \right). \end{aligned} \quad (9)$$

We close our system, Eqs. 2 and 9, by applying constraints (7) to eliminate the internal forces. Following algebraic manipulation, we derive the governing equations for $\ddot{\mathbf{X}}$ and $\ddot{\theta}$:

$$\begin{aligned} Fr \ddot{\mathbf{X}}(t) = & \int_0^1 \mathbf{F} ds \\ Fr \ddot{\theta}(t) = & -\frac{1}{J} \int_0^1 (\mathbf{X} - \bar{\mathbf{X}})^\perp \cdot \mathbf{F} ds \\ & + Fr \frac{1}{J} \int_0^1 I_0[\mathbf{X}_s^\perp] \cdot I_0[\mathbf{X}_s(\dot{\theta} + I_0[\kappa_t])^2] \\ & - I_0[\mathbf{X}_s] \cdot I_0[\mathbf{X}_s I_0[\kappa_{tt}]] ds \end{aligned} \quad (10)$$

where $J = \int_0^1 (\mathbf{X} - \bar{\mathbf{X}})^2 ds$ is the moment of inertia. The right hand side is a function of $\bar{\theta}$, $\dot{\theta}$, $\dot{\mathbf{X}}$ as well as the prescribed curvature κ and its derivatives. We turn to numerical solutions of Eq. 10.

4. Numerical Results. We observed that the body shape of a slithering snake can be well fit with the traveling wave of curvature

$$\kappa(s, t) = \epsilon \cos(k\pi(s + t)), \quad (11)$$

where $\epsilon = 7.0$ is the maximum radius of curvature of the snake and $k = 2.0$ its wavenumber. These numerical values for (ϵ, k) are used throughout our simulations unless otherwise specified.

We characterized how well a snake performs using two quantities of interest, the average speed in the x -direction and a mechanical efficiency:

$$\bar{U}_{avg} = \frac{1}{T} \int_0^T \bar{\mathbf{U}}(t) \cdot \hat{\mathbf{x}} dt \quad (12)$$

$$\eta = \frac{\mu_f \bar{U}_{avg}}{\frac{1}{T} \int_0^T \int_0^1 \mathbf{F} \cdot \dot{\mathbf{X}}(s, t) ds dt} . \quad (13)$$

Here, $T = 2/k$ is the period for the sinusoidal curvature given in Eq. 11 and $\bar{U} = \dot{\bar{\mathbf{X}}}$ is the speed of the center of mass. There are several ways to define efficiency. For a limbless organism in sliding, the minimum cost of transport, per mass of snake, is $\mu_f U_{avg}$, the power consumed while dragging a straight snake along the ground at a speed U . We define the efficiency η as the ratio of this minimum cost of transport to the snake's mechanical power dissipated during sliding. This ratio is inevitably less than unity because of the snake's serpentine path along the ground.

4.1. Numerical Techniques. Numerical integration of our system of Eqs. 10 is accomplished using a standard second-order Adams-Bashforth scheme. Integrals were evaluated to second order using the trapezoidal rule. A temporal and spatial resolution of $\Delta t = 10^{-3}$ and $\Delta s = 1/300$ were sufficient to obtain accurate results for $(\bar{X}, \bar{Y}, \bar{\theta})$. We assumed that steady-state was established when \bar{U}_{avg} changed by less than 1% between periods. Generally, we found that the virtual snake was found to relax to this steady-state within five periods when released with a speed of 1.

Among certain snake gaits, such as sidewinding, rectilinear, and concertina locomotion, the snake's belly clearly experiences points of instantaneous rest. We could not determine in our experiments of slithering whether points of the belly pass through rest. In fact, an assumption of our model is that no points on the snake's belly experience instantaneous rest, and so sliding friction, rather than static friction, is acting on the snake throughout its motion. This assumption was checked for consistency by determining whether any points on the snake were at rest during the simulation. We decided that rest occurred at a time t_0 if instantaneous velocities $U(t)$ and $V(t)$ along the snake both changed sign at t_0 . In our simulations, we found that static contact was experienced only for the lowest snake body speeds. This posed no problem for our modeling because we are interested in peak speed and efficiency, in which rest does not occur. Nevertheless, our model does not include the effects of static friction as its inclusion would be very complicating.

4.2. Results. We performed simulations of our kinematic model to characterize its predictions of peak speed and efficiency of slithering. We tested various waveforms and weight distributions in an *ad hoc* search of an "optimal" slithering gait. We also characterized snake speed in terms of the frictional properties of the underlying surface. We found in our simulations and experiments that snakes rarely slid backwards. Correspondingly, the backwards friction coefficient μ_b had little effect on our results and its effect on snake speed is not presented. Presumably, μ_b would become more important when the snake climbs uphill.

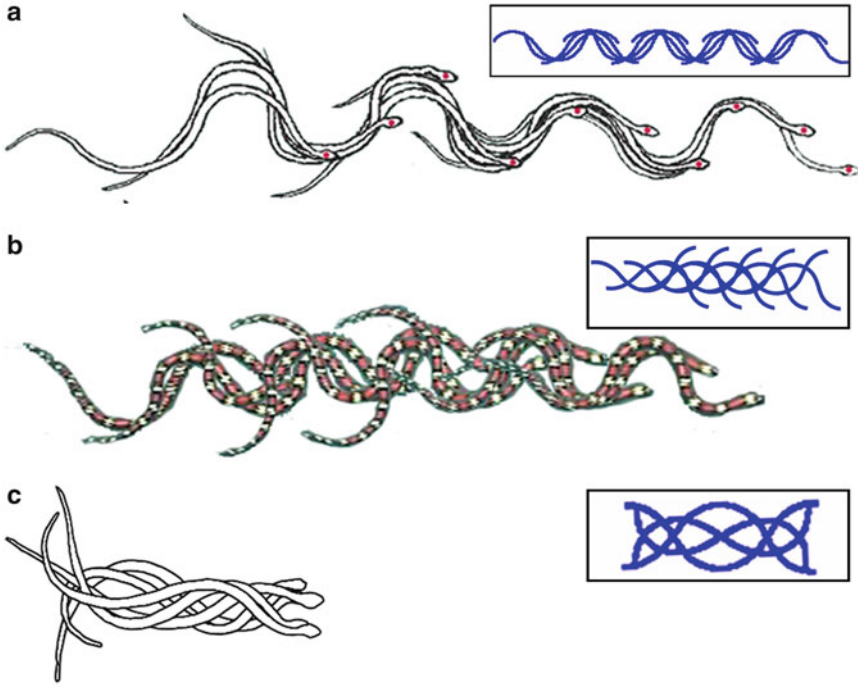


FIG. 5. Time-lapse trajectories of corn and milk snakes with insets of simulations. (a) During “sprinting” on cloth surfaces, both corn and milk snakes seem to be pushing off microscopic push-points, generating a trajectory with near perfect wave efficiency (with wave efficiency defined in Maladen et al. [29]). A nearly matching simulation is generated using $\mu_t = 10\mu_f$. (b) On the same cloth surface, and at more leisurely snake speeds, slipping is evident. Simulation is generated using $\mu_t = 2\mu_f$ and $A = 0.2$ in our weight-redistribution model. (c) On smooth fiberboard, the same milk snake slithers in place, advancing very slowly. Simulation is generated using $\mu_t = \mu_f$

Figure 5 shows time-lapse trajectories for three snakes from our experiments, which represent useful test cases for our model. Figure 5a shows a corn snake performing lateral undulation at high speed ($\bar{U} = 0.4$) on cloth. Milk snakes are also able to attain such high speeds, but we are unable to account for it with our kinematic model or its elaboration to include lifting, discussed below. However, a trajectory of a virtual snake with a high degree of anisotropy ($\mu_t/\mu_f = 10$; shown in inset at right) shows a qualitatively similar motion. Figure 5b shows a milk snake, again on cloth, moving more slowly. Slipping is clearly evident; we discuss the accompanying simulation for this snake in the next section. In Fig. 5c, the same snake performs poorly on a smooth fiberboard surface; it struggles in vain to move forward. On this surface the friction is nearly isotropic ($\mu_f = \mu_t$), and our model (inset at right) accounts well for the lack of forward motion. Clearly, snake motion is highly dependent on frictional anisotropy.

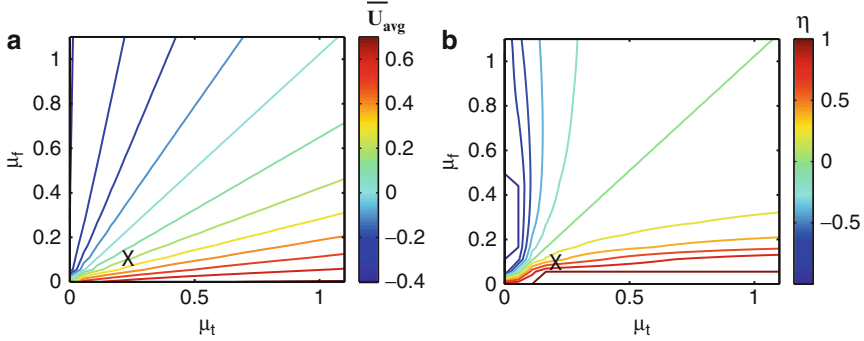


FIG. 6. Frictional dependence of speed and efficiency. The “X” represents the friction anisotropy measured for experiments of milk snakes on cloth

Figure 6a shows the virtual snake’s speed \bar{U}_{avg} over a range of friction coefficients μ_t and μ_f . The straight contour lines show that \bar{U}_{avg} depends essentially on the ratio of the friction coefficients, $An_{\perp} = \mu_t/\mu_f$, which is consistent with Eqs. 10 in the low Froude number limit. We examined friction coefficients between 0 and 1, the typical range of friction coefficients for dry solids [2, 45]. The snake geometry was fixed at $(k, \epsilon) = (2.0, 7.0)$, the values observed in our experiments. There are clearly two regimes in this contour plot, separated by the line $\mu_t = \mu_f$. Snakes below this line, for which $\mu_t > \mu_f$, move forward; snakes above this line, $\mu_t < \mu_f$, move in the opposite direction (backwards).

Figure 6b shows the mechanical efficiency η over a range of friction coefficients. For forward motion, we see that regions of high efficiency closely match those of high speed (Fig. 6a), as shown by the similarity in the two plots. Using the geometries observed for the milk snake on cloth, the efficiency of the virtual snake is $\eta = 0.25$. The highest possible speed is 0.6 for the highest frictional anisotropies, which corresponds to the snake moving near its wave speed.

Figure 7a shows the range of possible snake waveforms for $k < 10$ and $\epsilon < 20$. Figure 7b, c shows the speed and efficiency as a function of geometry for anisotropies of $An_{\perp} = 2$ and 10. For these numerical experiments, the forward friction coefficient μ_f is maintained constant at 0.1 and the transverse coefficient is increased (from 0.2 in Fig. 7a to 1.0 in Fig. 7b). The important features of these contour plots are the position and height of the peaks associated with maximum speed and efficiency. It is interesting that for an anisotropy of $An_{\perp} = 2$, there are two geometries

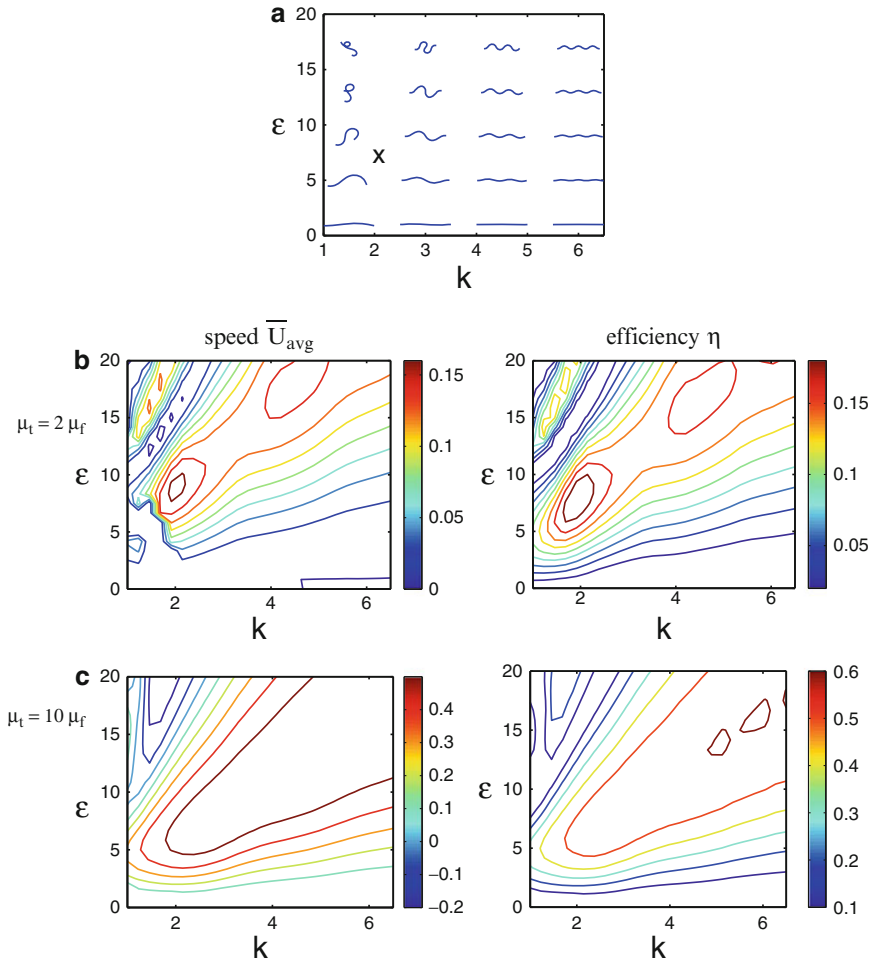


FIG. 7. Geometric dependence of speed and efficiency. (a) Range of snake waveforms as a function of k and amplitudes ϵ . Note that some at high ϵ are physically unrealizable due to body crossing. The “X” marks the observed snake waveform from our experiments. (b and c) Speed and efficiency for two levels of anisotropy. Dark blue regions occurring at the borders of the speed plots indicate where the snake body passes through a static position (zero speed in x and y directions). Here the model breaks down as static friction forces should then be generated, which we signify by making the body speed zero

associated with peak speed and efficiency: $(k, \epsilon) = (2, 8)$, as used here as characteristic of snakes, and $(\kappa, \epsilon) = (5, 18)$. As the anisotropy parameter is increased, these peaks coalesce.

These contour plots also reveal the regime of validity of our assumption of sliding contact. We find that certain slowly moving snakes exhibit

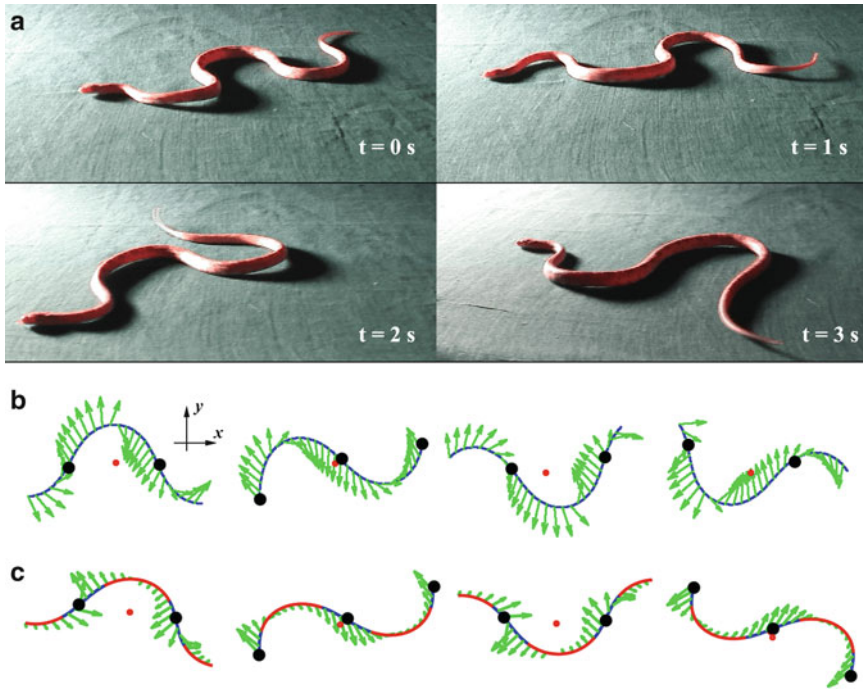


FIG. 8. (a) *Body-lifting during lateral undulation.* (b and c) *Visualization of the simulated propulsive forces on a virtual snake with uniform (b) and nonuniform (c) weight distribution.* Arrows indicate the direction and magnitude of the propulsive frictional force applied by the snake to the ground. Red lines indicate sections of the body with a normal force $N < 1$; the red dot indicates the center of mass. Inflection points of body shape, shown in black, show in (c) where the load is greatest. Note that in these simulations, although the weight distribution is nonuniform, the snake's body remains in contact with the ground everywhere along its body. (b and c) corrects the corresponding figures in Hu et al. [23]

points of rest, for which our model may not be accurate. These regions are indicated by having zero speed and efficiency (the dark blue areas). They occur at the borders of the contour plots, for snakes with either very low amplitude ϵ or very high wavenumber.

4.3. Weight Redistribution. Thus far, we have assumed that the snake presses its belly uniformly along the ground. This assumption appears to be false in several of our experiments on slithering and clearly in the sidewinding gait studied by other investigators. Figure 8 shows a snake lifting the peaks and troughs of its undulatory wave, while maintaining the majority of its body in sliding contact, as it slithers forward. It is possible that points of the snake pass through instantaneous rest. To consider the effects of a non-uniform weight distribution, we modify our friction force law, Eq. 8, by replacing the weight per unit length ρg by a normal force function $\rho g N(s/L, t/\tau)$. We investigate the effects of the snake unloading

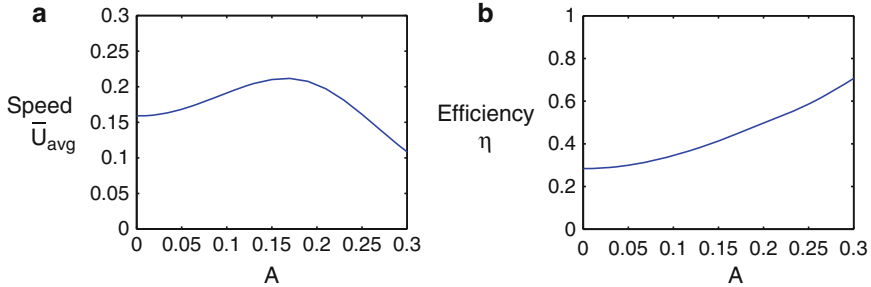


FIG. 9. The calculated speed and efficiency of the virtual snake as a function of the lifting amplitude A

its weight in these key areas by assigning its normal force to the approximate square wave centered at the snake’s peaks and troughs,

$$N(s, t) = \frac{e^{-A^2\kappa^2}}{\int_0^1 e^{-A^2\kappa^2} ds} \quad (14)$$

where the “unloading” parameter A gives qualitatively the “width” of the lifted region. This function increases normal force where curvature $\kappa = \epsilon \cos(k\pi(s + t))$ is zero (the inflection points) and lifts the snake at regions of high curvature (the peaks and troughs of the body wave). To explore the effect of this unloading parameter A , we first fix the snake’s geometry and anisotropy and change the degree the snake lifts. Figure 9 shows the dependence of the snake’s speed and efficiency on the unloading parameter A . We use the usual values for anisotropy and waveform ($An_{\perp} = 2$, $k = 2.0$ and $\epsilon = 7.0$). Moderate weight redistribution by the snake ($A = 0.2$) results in speeds of $\bar{U}_{avg} = 0.21$, which are 35% higher than the speeds at zero unloading. Moreover, redistributing weight causes efficiency to increase nearly up to 50% from $\eta = 0.3$ to 0.55 (see Fig. 9b, inset at right). Note that our definition of efficiency does not account for the cost of raising portions of the body.

5. Discussion. In summary, we have recorded and quantified the motion of snakes on various types of flat surfaces (smooth fiberboard and rough cloth) and developed mathematical models to account for surface texture inducing motion through anisotropic friction. We highlighted the use of dynamic body lifting in increasing locomotion speed and efficiency. By performing a brief optimization – scanning through A to maximize speed — we found that snakes can increase their speed up to 30% and efficiency by 50% by lifting their bodies as they slither.

In legged locomotion on flat rough surfaces, there is often little slipping, and small losses due to friction or air resistance [1]. As a result, metabolic energy is consumed by kinetic energy (swinging of the limbs)

and gravitational energy (vertical motion of center of mass). Gaits (walking or running) are chosen according to the ratio of kinetic to gravitational energies [1]. Snake locomotion is quite different because sliding is of utmost importance. Froude numbers are always low, indicating that inertia is negligible compared to friction. Center of masses do not change appreciably in height, unless the snake lifts its body. In our study, we were able to predict the motion of the body by keeping track of the forces resisting and the energy dissipated during sliding.

The efficacy of snake locomotion is highly dependent on the medium the snake moves upon. For example, snakes on smooth surfaces such as hard fiberboard cannot slither forward because their scales can generate insufficient frictional anisotropy. We note that most snakes will quickly learn to rely on their other gaits (or lift their bodies) if slithering does not avail them. We also observed that snakes can slither as quickly on cloth as on peg boards. This is because the asperities in the ground act as microscopic push points to the snake's scales. The idea that snakes can use microscopic push points is a new one and bears consideration in modeling of snakes on all surfaces, not just flat ones.

The anatomical structure and physiological responses of snakeskin is very crudely captured in our model and friction experiments. We include no abilities of the skin to actively modulate its friction. For example, when the trunk of the snake bends, the scales reorient themselves with respect to each other, thus changing their contact orientation with the ground. Moreover, anatomical observations [4, 11] suggest that snakes also have control over individual scales. Modeling features such as these may be necessary to fully account for the range of observed snake speeds.

Our numerical method complemented our experiments, particularly for understanding the effect of body-lifting. Weight redistribution is difficult to experimentally quantify, and we were only able to roughly do so when the degree of lifting was extreme. Use of a photoelastic gelatin, as has been done to study cockroach locomotion [14], is too adhesive for snakes to move naturally (nonetheless, see Fig. 10). The deployment of arrays of small pressure sensors might be useful in this regard.

Can a human ever move like a snake? Infants, who must learn to crawl and eventually walk, begin their motile lives with an inch-worming motion. A full body-suit allowing an adult to slither must reduce abrasive wear and provide frictional anisotropy. There are a number of man-made devices that rely on frictional anisotropy, such as roller-blades and ice skates. Certain toys resembling two skateboards linked together allow one to shuffle one's legs, creating a traveling wave. Coordinated motion of several people standing on a series of devices may generate a sufficiently long traveling wave so as to look snake-like.

Body-lifting shows that limbless locomotion can have similarities to walking. Shifting weight from the left to the right side of the body is a common strategy for legged locomotion, as animals clearly prefer to lift



FIG. 10. *A snake attempting to slither on photoelastic gelatin. The luminescent areas indicate regions of highest applied force*

rather than drag their legs. It also appears to be important for snakes, as shown by our predictions of large gains in speed and efficiency. However, we also did not estimate the internal energetic costs of lifting the body, for example, as is expended by a weight-lifter to hold a static load. For large snakes, this may account for a large portion of the energy budget. Such considerations will be especially important for snake-like robots, whose batteries will likely make them heavier than their natural counterparts, and for whom efficiency will be of the utmost importance.

Supplementary Movies.

- Movie 1. A corn snake slithering on cloth. Previous models on snake locomotion could not account for the forward motion of the body because there are no apparent push points for the snake's flanks. Body length, 30 cm. http://youtu.be/urhXl_prdKE.
- Movie 2. A corn snake slithering in place on smooth fiberboard. The snake is unable to slither forward because its scales cannot gain purchase. <http://youtu.be/YYAmN11YtzQ>.
- Movie 3. This sequence of videos shows a milk snake slithering up a cloth-covered incline, increased from 0° to 12° . At 7° of inclination the snake slithers in place, and at higher inclinations, slides backwards. <http://youtu.be/U3qH8hcHZos>.
- Movie 4. Viewing a slithering corn snakes from the side, we see that they may lift parts of the body from the ground. The snake's weight is concentrated on the remaining areas of contact. When we incorporated this behavior into our theoretical model, we found increases in both body speed and efficiency. <http://youtu.be/rfba0JY31HI>.

Acknowledgements. We acknowledge Grace Pryor, Jasmine Nirody and Terri Scott for assistance with experiments. This work was partially supported by the Lilian and George Lyttle Chair in Applied Mathematics. DLH acknowledges the support of NSF grant PD08-7246.

REFERENCES

- [1] Alexander RM (2003) Principles of animal locomotion. Princeton University Press, Princeton.
- [2] Avallone EA, Baumeister T III (eds) (1996) Marks' standard handbook for mechanical engineers. McGraw-Hill, New York, pp 3–23
- [3] Bellairs A (1970) Life of reptiles, vol 2. Universe books, New York, pp 283–331.
- [4] Buffa P (1905) Ricerche sulla muscolatura cutanea dei serpenti e considerazioni sulla locomozione di questi animali. *Atti Acad Ven Trent* 1:145–237
- [5] Burdick JW, Radford J, Chirikjian GS (1993) A 'sidewinding' locomotion gait for hyper-redundant robots. In IEEE international conference on robotics and automation, Los Alamitos, CA, pp 101–106
- [6] Bush JWM, Hu DL (2006) Walking on water: biolocomotion at the interface. *Ann Rev Fluid Mech* 38:339–369
- [7] Chan B, Balmforth N, Hosoi A (2005) Building a better snail: lubrication and adhesive locomotion. *Phys Fluids* 17:113101
- [8] Chernousko FL (2003) Snake-like locomotions of multilink mechanisms. *J Vib Cont* 9:235–256
- [9] Childress S (1981) Mechanics of swimming and flying. Cambridge University Press, Cambridge
- [10] Choset HM (2005) Principles of robot motion: theory, algorithms and implementation. MIT Press, Cambridge
- [11] Cundall D (1987) Functional morphology. In: Siegel RA, Collins JT, Novak SS (eds) Snakes: ecology and evolutionary biology. Blackburn press, Caldwell NJ, pp 106–140
- [12] Dorgan KM, Jumars PA, Johnson B, Boudreau BP, Landis E (2003) Burrow elongation by crack propagation. *Nature* 433:475
- [13] Ernst CHZ, Zug GR (1996) Snakes in question. Smithsonian, Washington, DC
- [14] Full R, Yamauchi A, Jindrich D (1995) Maximum single leg force production: Cockroaches righting on photoelastic gelatin. *J Exp Biol* 198:2441–2452
- [15] Gans C (1962) Terrestrial locomotion without limbs. *Amer Zool* 2:167–182
- [16] Gasc JP, Gans C (1990) Tests on locomotion of the elongate and limbless lizard *anguis fragilis* (Squamata: Anguillidae), *Copeia*, pp 1055–1067
- [17] Gray J (1946) The mechanism of locomotion in snakes. *J Exp Biol* 23:101–120
- [18] Gray J, Lissman HW (1950) The kinetics of locomotion of the grass-snake. *J Exp Biol* 26:354–367
- [19] Guo ZV, Mahadevan L (2008) Limbless undulatory locomotion on land. *Proc Natl Acad Sci U S A* 105:3179–3184
- [20] Hazel J, Stone M, Grace MS, Tsukruk VV (1999) Nanoscale design of snake skin for reptation locomotions via friction anisotropy. *J Biomech* 32:477–84
- [21] Heckrote C (1967) Relations of body temperature, size and crawling speed of the common garter snake, *Thamnophis s. sirtalis*. *Copeia* 4:759–763
- [22] Hirose S (1993) Biologically inspired robots: snake-like locomotors and manipulators. Oxford University Press, Oxford.
- [23] Hu DL, Nirody J, Scott T, Shelley MJ (2009) The mechanics of slithering locomotion. Proceedings of the national academy of sciences, USA, 106:10081–10085
- [24] Jayne BC (1986) Kinematics of terrestrial snake locomotion. *Copeia* 22:915–927.
- [25] Juarez G, Lu K, Sznitman J, Arratia P (2010) Motility of small nematodes in wet granular media. *Europhys Lett* 92:44002
- [26] Jung S (2010) *Caenorhabditis elegans* swimming in a saturated particulate system. *Phys Fluids*, 22:031903
- [27] Lissman HW (1950) Rectilinear locomotion in a snake (*Boa occidentalis*). *J Exp Biol* 26:368–379
- [28] Mahadevan L, Daniel S, Chaudhury MK (2004) Biomimetic ratcheting motion of a soft, slender, sessile gel. *Proc Natl Acad Sci U S A* 101:23–26

- [29] Maladen R, Ding Y, Li C, Goldman D (2009) Undulatory swimming in sand: subsurface locomotion of the sandfish lizard. *Science* 325:314
- [30] Marvi H, Hu D (2012) Friction Enhancement in Concertina Locomotion of Snakes. *Journal of the Royal Society Interface* (In Press)
- [31] Miller G (2002) Snake robots for search and rescue. In: Ayers JDJ, Rudolph A (eds) *Neurotechnology for biomimetic robots*. Bradford/MIT Press, Cambridge, pp 269–284
- [32] Moon BR, Gans C (1998) Kinematics, muscular activity and propulsion in gopher snakes. *J Exp Biol* 201:2669–2684
- [33] Mosauer W (1932) On the locomotion of snakes. *Science* 76:583–585
- [34] Mosauer W (1935) How fast can snakes travel? *Copeia* 1935:6–9
- [35] Netting MG (1940) Size and weight of a boa constrictor. *Copeia* 4:266
- [36] Ostrowksi J, Burdick J (1996) Gait kinematics for a serpentine robot. In: IEEE international conference on robotics and automation, Minneapolis, minnesota, pp 1294–1299
- [37] Rachevsky N (1938) *Mathematical biophysics: physico-mathematical foundations of biology*, vol 2. Dover, New York, pp 256–261
- [38] Renous S, Hoffing E, Gasc JP (1995) Analysis of the locomotion pattern of two microteiid lizards with reduced limbs, *Calyptommatus leiolepis* and *Nothobachia ablephara* (Gymnophthalmidae). *Zoology* 99:21–38
- [39] Secor SM, Jayne BC, Bennett AC (1992) Locomotor performance and energetic cost of sidewinding by the snake *crotalus cerastes*. *J Exp Biol* 163:1–14
- [40] Summers AP, O'Reilly JC (1997) A comparative study of locomotion in the caecilians *Dermophis mexicanus* and *Typhlonectes natans* (Amphibia: Gymnophiona). *Zool J Linn Soc* 121:65–76
- [41] Teran J, Fauci L, Shelley M (2010) Viscoelastic fluid response can increase the speed and efficiency of a free swimmer. *Phys Rev Lett* 104:038101
- [42] Tong J, Ma Y-H, Ren L-Q, Li J-Q (2000) Tribological characteristics of pangolin scales in dry sliding. *J Mater Sci Lett* 19:569–572
- [43] Trueman ER (1975) *The locomotion of soft-bodied animals*. Edward Arnold, London
- [44] Walton M, Jayne BC, Bennett AF (1990) The energetic cost of limbless locomotion. *Science* 249:524–527
- [45] Zmitrowicz A (2006) Models of kinematics dependent anisotropic and heterogenous friction. *Int J Solids Struct* 43:4407–4451